Solvated Interaction Energy (SIE) for Scoring Protein−Ligand Binding Affinities. 1. Exploring the Parameter Space

Marwen Naïm,[†,⊥] Sathesh Bhat,[†,‡,Δ] Kathryn N. Rankin,[†,#,§] Sheldon Dennis,[†] Shafinaz F. Chowdhury,[†,⊥] Imran Siddiqi,[†,▽] Piotr Drabik,[†,○] Traian Sulea,[†] Christopher I. Bayly,[§] Araz Jakalian,[∥] and Enrico O. Purisima*[,†,‡]

Biotechnology Research Institute, National Research Council of Canada, 6100 Royalmount Avenue, Montreal, Quebec, Canada H4P 2R2, Department of Biochemistry, McGill University, Montreal, Quebec, Canada H3G 1Y6, Merck Frosst Canada & Co., 16711 Trans Canada Hwy., Kirkland, Quebec, Canada H9H 3L1, Boehringer Ingelheim (Canada) Ltd., 2100 Cunard Street, Laval, Quebec, Canada H7S 2G5

Received September 19, 2006

We present a binding free energy function that consists of force field terms supplemented by solvation terms. We used this function to calibrate the solvation model along with the binding interaction terms in a self-consistent manner. The motivation for this approach was that the solute dielectric-constant dependence of calculated hydration gas-to-water transfer free energies is markedly different from that of binding free energies (*J. Comput. Chem*. **2003**, *24*, 954). Hence, we sought to calibrate directly the solvation terms in the context of a binding calculation. The five parameters of the model were systematically scanned to best reproduce the absolute binding free energies for a set of 99 protein−ligand complexes. We obtained a mean unsigned error of 1.29 kcal/mol for the predicted absolute binding affinity in a parameter space that was fairly shallow near the optimum. The lowest errors were obtained with solute dielectric values of $D_{in} = 20$ or higher and scaling of the intermolecular van der Waals interaction energy by factors ranging from 0.03 to 0.15. The high apparent D_{in} and strong van der Waals scaling may reflect the anticorrelation of the change in solvated potential energy and configurational entropy, that is, enthalpy−entropy compensation in ligand binding (*Biophys. J.* **2004**, *87*, 3035−3049). Five variations of preparing the protein−ligand data set were explored in order to examine the effect of energy refinement and the presence of bound water on the calculated results. We find that retaining water in the final protein structure used for calculating the binding free energy is not necessary to obtain good results; that is the continuum solvation model is sufficient. Virtual screening enrichment studies on estrogen receptor and thymidine kinase showed a good ability of the binding free energy function to recover true hits in a collection of decoys.

INTRODUCTION

The reliable prediction of protein−ligand binding free energies is essential for successful structure-based drug design as well as for understanding the thermodynamic determinants of molecular recognition. Because binding affinity is utilized as a criterion for ligand selection in drug discovery processes, the past few years have seen a number of binding affinity prediction methods emerge to address the "scoring problem". These methods range from rapid quantitative structure−activity relationship based (empirical) scoring functions to the more ambitious and rigorous free energy perturbation and linear response methods.[1−7]

An emergent group of methods that represent a reasonable compromise between time, computational resources, and accuracy combines molecular mechanics force fields with a continuum treatment of solvation. Continuum electrostatics solvation models replace the solvent by a dielectric continuum but retain an atomic-level description of the solute. These methods combine terms that describe electrostatic contributions to solvation, for example, through the generalized Born (GB) or Poisson−Boltzmann methods, with terms that describe the nonpolar contribution to solvation, that is, van der Waals interaction with the solvent and cavity formation. These continuum solvation models contain parameters that have traditionally been parametrized to fit experimental solvation free energies obtained for small organic molecules. This is a potential cause for concern because we showed in previous work that parametrizing the electrostatic component of a continuum solvation model against hydration transfer free energies of small molecules does not automatically guarantee transferability of the fitted parameters to binding free energy calculations.[8] As proposed in that work, we now extend the analysis and present the parametrization of a continuum solvation model based directly on experimental binding data. We first incorporated

* Corresponding author phone: (514) 496-6343; fax: (514) 496-5143; e-mail: enrico.purisima@nrc.ca.
† National Research Council of Canada.
‡ McGill University.
§ Merck Frosst Canada & Co.
∥ Boehringer Ingelheim (Canada) Ltd.
⊥ Current address: Lady Davis Institute for Medical Research, McGill University, Montreal, Quebec.
Current address: University of Alberta.
▽ Current address: Central Drug Research Institute, Council of Scientific and Industrial Research of India, Lucknow-226001, India.
○ Current address: NINT, NRC, Edmonton, Alberta.
Δ Current address: Merck Frosst Canada & Co.

10.1021/ci600406v CCC: $37.00
Published on Web 01/05/2007

the continuum electrostatics solvation into a binding affinity model and then profiled the fitness of the latter in the space of its varying parameters.

In a similar study, Zou and co-workers recently described the incorporation and calibration of a GB/surface area (SA) solvation model into the DOCK program.[9] They systematically varied three parameters—a scale factor for the Lennard-Jones potential and two surface area coefficients—and analyzed the effect on mean error in predicting binding affinities. In this work, we carried out a more extensive exploration of parameter space. Aside from coefficients for the van der Waals interaction energy and buried surface area, we also calibrated the solute interior dielectric constant and atomic radii using the boundary element Poisson equation solver, BRI BEM, for solvation electrostatics.[10,11] We carried out a systematic study of how well various combinations of the electrostatic and nonelectrostatic solvation parameters, in conjunction with the AMBER force field,[12] could reproduce experimental binding free energies for a diverse set of 99 complexes containing protein−small-molecule and protein−peptide interactions. All these complexes have known crystal structures, thus decoupling the docking problem from the problem of predicting binding affinity. The effect of the protocol of energy minimization and inclusion of structural water molecules on the calibrated parameters was also investigated. The uniqueness, physical significance, and system transferability of optimal parameters are discussed. As a validation of the parameters, virtual screening enrichment studies were carried out for estrogen receptor (ER) and thymidine kinase (TK), neither of which was in the original training set.

METHODS

Data Set. Our starting point for building the present data set was based on the content of nine scoring function data sets (i.e., *Chemscore*, *Score1*, *Score2*, *Autocock*, *Validate*, *Hammerhead*, *Drugscore*, *PMF*, and *Gold*), six of which were reported by Brooks and co-workers.[13] After removing redundancies, we ended with 238 X-ray complexes representing 102 different proteins. One limitation to this set is that the average number of complexes per target was around two, which did not allow us to observe target-specific trends or artifacts in our calculated binding free energies. In order to retrieve additional protein−ligand X-ray complexes per protein target, we searched the Protein Data Bank (PDB) database using the keywords "complex" or "bound" to pull out related protein−ligand complexes. With few exceptions, we retained only protein targets having six or more such PDB entries. The selected proteins were classified according to the International Union of Biochemistry and Molecular Biology nomenclature (http://www.chem.qmul.ac.uk/iubmb/). A total of 47 subclasses were found.

The collected complexes were submitted to a preliminary curation. First, the protein sequence of each complex was aligned to the corresponding wild type, because some mutations are simply not reported in the PDB header. Their crystal structures were visually inspected in Sybyl (Tripos Inc., St. Louis, MO) in order to (i) locate missing peptide fragments and side chains not reported in the PDB header and (ii) assign the category and binding mode of the ligand, for example, covalent or noncovalent and peptidyl or nonpeptidyl. Only noncovalent complexes were considered in the present data set.

This led to a data set containing 925 crystal structures. From this, we selected 15 targets that had six or more representative protein−ligand crystal structures and for which we could find the corresponding binding affinity data in the literature. From these, only complexes with available inhibition (K_i) or dissociation constants (K_d) were considered. In cases where multiple binding constants could be located in the published literature, the geometric mean of those values was taken as the experimental value in the present study. IC_{50} data were excluded to avoid any ambiguity in the conversion to K_i. This yielded a data set of 138 structures. A total of 32 of these complexes contained metals directly interacting with the ligands. These were removed from consideration because of known difficulties in modeling metal−ligand interactions. Also set aside initially were seven complexes in which the target and the ligands had net charges of opposite sign. Such complexes have been observed to exhibit a different electrostatic dependence on the internal dielectric constant as compared to complexes with net charges of the same sign or in which at least one of the two partners is neutral.[14] We were left with 11 targets comprising 99 complexes. A list of the PDB codes and protein targets is given in Table S1 (Supporting Information). In these complexes, the target and ligand had net charges of the same sign or at least one was neutral. All the selected structures were submitted to a consistent and well-defined preparation procedure.

Protein Structure Preparation. The 3D coordinates of proteins within the same target subset were structurally aligned to a common orientation using Sybyl. This facilitated the reconstruction of peptide fragments and side chains missing in some of the deposited crystal structures because of poorly defined electron density maps. The missing fragment was normally imported from a better-resolution crystal structure of the same protein. The program Reduce[15] was used to add hydrogen atoms to the protein structure and optimize the orientation of polar hydrogens. Alternate tautomeric states of imidazole groups were explored as well as flipping of carbonyl and amide positions in Gln and Asn side chains.

The side-chain ionization states were based on the pK_a of the free amino acid and the pH of the assay rather than the pH of the crystal structure determination. We chose to go with the binding assay pH because the measured affinities are probably more sensitive to the pH than the structure is. When the binding assay pH was less than or equal to 6.0, that is, the pK_a of histidine, the side chain was considered to be protonated. In some cases where the histidine side chain could form a salt bridge, we considered it protonated even at higher pH. For HIV protease, Asp25 in chain A was protonated while the corresponding Asp25 in chain B was ionized. Some water molecules were kept within the crystal structure if they seemed to be likely involved in a network of hydrogen bonds either in the core of the protein or between the ligand and protein. Generally, water hydrogen atom coordinates were not present in the deposited structure in PDB. We then added them through Sybyl and manually adjusted their orientation to optimize possible hydrogen bonds with neighboring polar atoms.

Ligand Force-Field Parameters. The ligands were extracted from X-ray complexes and visually inspected in Sybyl for proper atom-type and bond-order assignment. In many cases, manual correction was necessary because of incorrect atom- and/or bond-type assignment. The structures were then used to generate general AMBER force field (GAFF) atom types using the antechamber module of AMBER.[16] This facility automatically generates parameters that are compatible with the AMBER force field (atom types, bond stretch, angle bend, and torsional and improper torsional parameters). The automatically assigned GAFF atom types were then manually checked and corrected as necessary. For example, in our hands, antechamber tends to assign an sp^3 GAFF atom type to amidinium nitrogens of benzamidines; these were manually changed to the appropriate sp^2 GAFF atom type.

Partial charges for the ligands were calculated by an iterative protocol of restrained AMBER energy minimization and two-stage restrained-fitting procedure (RESP)[17] to the single-point Hartree−Fock 6-31G* electrostatic potential calculated using GAMESS.[18] Initial Gasteiger partial charges were assigned to the ligand, which was then energy-minimized by itself to a root-mean-square (RMS) gradient of 0.05 kcal/mol·Å with a 0.5 kcal/mol·Å^2 harmonic force-constant restraint on the coordinates of the non-hydrogen atoms to maintain the bound conformation. RESP charges were then calculated for the energy-minimized structure. When the updated partial charges were used, the energy minimization−charge fitting procedure was iterated two more times (without the coordinate constraints) to obtain the final charge set. In a virtual screening pipeline, this procedure can be replaced by the more rapid AM1−BCC method of assigning partial charges.[19]

Preparation of the Protein−Ligand Complex. In order to investigate the effect of energy-refinement as well as the presence of structural water on our calculated binding free energies, we prepared five versions for each complex.

(*i*) *Version 1.* Constrained energy minimization was carried out on the protein−ligand complexes, including retained structural water molecules, with the AMBER force field supplemented by ligand GAFF parameters with a distance-dependent dielectric constant ($4r_{ij}$) and an 8 Å nonbonded cutoff to an RMS gradient of 0.01 kcal/mol·Å. Only hydrogen atoms were relaxed through this energy minimization; that is, all non-hydrogen atoms remained at their crystal structure positions. The van der Waals parameters for metal ions (Mg^{2+}, Ca^{2+}, and Zn^{2+}), if present, were adapted from Åqvist.[20]

(*ii*) *Version 2.* Water molecules were removed from the final structure of version 1.

(*iii*) *Version 3.* Restrained energy minimization of all ligand atoms along with protein hydrogen atoms within 4 Å of the ligand in the final structure of version 2 was carried out. A harmonic force constant constraint of 3 kcal/mol·Å^2 was applied to the ligand non-hydrogen atoms.

(*iv*) *Version 4.* With the same starting point as version 1 being used, hydrogen atoms were relaxed through energy minimization while the non-hydrogen atoms were restrained to their crystallographic positions with a harmonic potential of 1 kcal/mol·Å^2.

(*v*) *Version 5.* All water molecules were removed from the final structure of version 4.

Binding Free Energy Expression and Models. The target−ligand binding free energy is approximated using the solvated interaction energy (SIE) formalism.

$$\Delta G_{\text{bind}}^{\text{calc}} = \underbrace{E_{\text{inter}}^{\text{C}} + \Delta G_{\text{bind}}^{\text{R}}}_{\Delta G_{\text{bind}}^{\text{elec}}} + \underbrace{E_{\text{inter}}^{\text{vdw}} + \Delta G_{\text{bind}}^{\text{npsol}}}_{\Delta G_{\text{bind}}^{\text{np}}} \quad (1)$$

$E_{\text{inter}}^{\text{C}}$ and $E_{\text{inter}}^{\text{vdw}}$ are the intermolecular Coulomb and van der Waals interaction energies in the bound state, respectively. The electrostatic contribution of the solvation free energy to binding, $\Delta G_{\text{bind}}^{\text{R}}$, is the change in the reaction field energy between the bound and free states. The nonpolar contribution of the solvation free energy to binding, $\Delta G_{\text{bind}}^{\text{npsol}}$, is the change in the nonelectrostatic solvation free energy (i.e., the solute−water van der Waals energy plus the cavitation cost in water) between the bound and free states. The target−ligand complex represents the bound state of the system, whereas the free, unbound state is obtained by infinite rigid separation of the ligand and target from the complex. The terms in eq 1 can be grouped into the electrostatic and nonpolar contributions to binding, $\Delta G_{\text{bind}}^{\text{elec}}$ and $\Delta G_{\text{bind}}^{\text{np}}$, respectively. Not included in eq 1 is the change in solute entropy upon binding, that is, changes in conformational, translational, and rotational entropy. Also, because we are using a rigid infinite separation model of binding, internal energies of neither the protein nor the ligand are taken into account.

The energy terms, $E_{\text{inter}}^{\text{C}}$ and $E_{\text{inter}}^{\text{vdw}}$, were calculated using the AMBER molecular mechanics force field without a nonbonded cutoff and with a dielectric constant, D_{in}, that was systematically scanned in the fitting procedure. The electrostatic solvation contribution, $\Delta G_{\text{bind}}^{\text{R}}$, was calculated using the continuum dielectric model with a solute interior dielectric constant, D_{in}, and a solvent dielectric constant of 78.5. Reaction field energies were computed by solving the Poisson equation with the boundary element method program, BRI BEM,[10,11] with a molecular surface generated with a variable-radius solvent probe using a marching tetrahedra algorithm.[21,22] Solute atoms were assigned scaled AMBER van der Waals radii, except for polar hydrogen atoms, for which no scaling was applied. Born radii for metal ions (Mg^{2+}, Ca^{2+}, and Zn^{2+}) were calculated from their experimental hydration free energies using the Born formula for a spherical solute cavity and were not scaled during parametrization. Partial atomic charges for the protein and water atoms were taken from the AMBER charge set, whereas ligands and, in some systems, cofactors were assigned RESP ab initio charges (described in the previous section).

The cavitation cost was taken to be proportional to the change in molecular surface area, ΔSA. We use the solvent-excluded surface rather solvent-accessible surface for the surface area calculation because it has been shown to better capture the details of the cavitation free energy as a function of intermolecular separation.[23] The change in solute−water van der Waals interactions can be calculated in two ways. It can be incorporated in the surface area calculation and subsumed in the resulting surface area proportionality factor, γ.

$$\Delta G_{\text{bind}}^{\text{npsol}} = \gamma \cdot \Delta \text{SA} \quad (2)$$

Alternatively, the solute−solute van der Waals interaction energy can be scaled by a linear factor β, reflecting a loss of solute−solvent van der Waals interactions for every solute−solute interaction formed, leading to

$$\Delta G_{\text{bind}}^{\text{npsol}} = (\beta - 1)E_{\text{inter}}^{\text{vdw}} + \gamma \cdot \Delta\text{SA} \quad (3)$$

One caveat in using eq 3 is that, if the ligand has clashes with the target leading to strong repulsive van der Waals interactions, there will be an artifactual, large favorable contribution from the calculated value of the "loss" of solute−solvent interactions. Also, in fitting parameters with terms incorporating eq 3, the surface area term will inevitably contain some of the solute−solvent van der Waals contributions.

Parametrization Methodology. Given a collection of protein−ligand complexes with a fixed set of partial charges, and force-field parameters, the binding free energies calculated using eq 1 depend on a number of variables. First, the choice of atomic radii used to construct the molecular surface defining the dielectric interface affects both the reaction field energy and surface-area-dependent nonpolar solvation energy terms. Second, the value of the solute dielectric, D_{in}, influences both the Coulomb interaction energy and the reaction field energy. Finally, the scaling factor for the surface area and/or van der Waals term affects the nonpolar contribution.

Thus, the calculated binding free energy, $\Delta G_{\text{bind}}^{\text{calc}}$, can be expressed as a function of solute atomic radii $\{r_i\}$, interior dielectric constant D_{in}, SA linear scaling coefficient γ, van der Waals interaction energy linear scaling coefficient β, and a fitting constant C.

$$\Delta G_{\text{bind}}^{\text{calc}}(\{r_i\},D_{\text{in}},\beta,\gamma,C) = E_{\text{inter}}^{\text{C}}(D_{\text{in}}) + \Delta G_{\text{bind}}^{\text{R}}(\{r_i\},D_{\text{in}}) + \beta \cdot E_{\text{inter}}^{\text{vdw}} + \gamma \cdot \Delta\text{SA}(\{r_i\}) + C \quad (4)$$

The parameter dependencies in eq 4 were analyzed using a systematic variation of the $(\{r_i\},D_{\text{in}},\beta,\gamma)$ parameters within physically meaningful ranges. The dependence of the binding free energy on the atomic radii was explored by linearly scaling the AMBER van der Waals radii

$$r_i = \rho \cdot r_i^{\text{AMBER}} \quad (5)$$

except for polar hydrogen radii (e.g., water, amide, hydroxyl, and thiol hydrogen atoms), which were kept fixed at a value of 1 Å, and ammonium hydrogen radii were increased to a fixed radius of 1.1 Å. The coefficient, ρ, was varied between 0.800 and 1.100 in increments of 0.025. No scaled or unscaled atomic radius was allowed to be less than 1 Å in order to avoid numerical instability in the boundary element calculation of the reaction field energy. D_{in} was varied between 1.0 and 20.0 in 29 uneven increments that sampled the low-dielectric region more (1.0, 1.2, 1.4, 1.6, 1.8, 2.0, 2.25, 2.5, 2.75, 3.0, 3.25, 3.5, 3.75, 4.0, 4.25, 4.5, 4.75, 5.0, 5.25, 5.5, 6.0, 6.5, 7.0, 7.5, 8.0, 9.0, 10, 13, and 20). At each combination of ρ and D_{in}, optimal γ, β, and C values were derived in a fitting process to best reproduce the experimental binding energies. Thus, a binding affinity model with five parameters (ρ, D_{in}, γ, β, and C) emerges:

$$\Delta G_{\text{bind}}^{\text{calc}}(\rho,D_{\text{in}},\beta,\gamma,C) = E_{\text{inter}}^{\text{C}}(D_{\text{in}}) + \Delta G_{\text{bind}}^{\text{R}}(\rho,D_{\text{in}}) + \beta \cdot E_{\text{inter}}^{\text{vdw}} + \gamma \cdot \Delta\text{SA}(\rho) + C \quad (6)$$

A total of 435 ρ and D_{in} combinations were examined along with the corresponding optimized β, γ, and C values.

In order to evaluate the fitness of a particular binding affinity model at varying combinations of the corresponding parameter set $\{p_i\}$, we defined an error function, err, as the mean absolute error between the calculated binding free energies and the experimental binding free energies for the M complexes in a data set.

$$\text{err}(\{p_i\}) = \frac{1}{M}\sum_{i=1}^{M} |\Delta G_{\text{bind}}^{\text{calc}}(\{p_i\}) - \Delta G_{\text{bind}}^{\text{exp}}| \quad (7)$$

For a given ρ and D_{in} combination, a least-squares fit was carried on the remaining parameters of interest, for example, β, γ, and C for eq 6. The resulting values from the least-squares fit were then used as the starting point for minimization of the mean absolute deviation, eq 7. The motivation for using the mean absolute deviation is that it is less sensitive than least-squares linear regression to the influence of outliers. Also calculated for each parameter combination obtained from the fitting procedure is the Spearman R correlation coefficient, which measures how well rank order is preserved in the data sets.[24] All parameter fitting calculations were carried out using the R statistics software.[25]

RESULTS AND DISCUSSION

Effect of Structure Preparation. Table 1 lists the parameters and mean absolute errors obtained with eq 6 for the five different protocols of structure preparation. The results show that the mean absolute deviation is not overly sensitive to the protocol of structure preparation with mean absolute errors ranging from 1.29 to 1.40 kcal/mol. These values are comparable with those afforded by current state-of-the-art binding affinity scoring functions.[26] Nevertheless, it appears that restrained energy minimization of the ligand in the rigid protein binding site (version 3) provides slightly better results over the other structural refinement protocols. Moreover, the presence or absence of structural water molecules in the final complex used for binding affinity calculation does not seem to have much influence on the quality of fit. In fact, the best fit is obtained when the water molecules are stripped away before making the final calculation. This is fortunate since deciding which water molecules to keep is not simple, and it is much easier to replace all water molecules with a continuum solvent. Figure 1 shows a scatter plot of the experimental versus the calculated binding free energies using eq 6 and version 3 of preparing the protein−ligand data set. We see generally good agreement over the entire data set as well within most of each protein target. Unless otherwise stated, for the rest of the discussion, we will be using version 3 of preparing the protein−ligand data set. The mean absolute error for version 3 is 1.29 kcal/mol for the optimized parameter set. The Spearman R value of 0.854 indicates that ranking of binding affinities is also well-preserved for the set as a whole. As a point of reference, the mean absolute error for the null hypothesis, that is, taking the average of the experimental

Table 1. Calibration of Binding Affinity Models on a Data Set Consisting of 99 Complexes from 11 Protein Targets[a]

energy minimization	structural water	err	β	γ	ρ	D_{in}	C
$E^{C}_{inter}(D_{in}) + \Delta G^{R}_{bind}(\rho,D_{in}) + \beta\cdot E^{vdw}_{inter} + \gamma\cdot\Delta SA(\rho) + C$							
Hs	no	1.35	0.008	0.013	0.800	20	−2.15
Hs	yes	1.38	0.027	0.012	0.750	20	−1.80
ligand/Hs	no	1.29	0.025	0.011	0.800	20	−2.23
complex	no	1.31	0.070	0.007	0.775	20	−2.26
complex	yes	1.40	0.082	0.006	0.750	20	−2.16
$E^{C}_{inter}(D_{in}) + \Delta G^{R}_{bind}(\rho,D_{in}) + \beta\cdot E^{vdw}_{inter}$							
Hs	no	1.68	0.147		1.000	20	−1.88
Hs	yes	1.69	0.148		0.825	20	−2.51
ligand/Hs	no	1.44	0.142		0.850	20	−2.40
complex	no	1.35	0.141		0.800	20	−2.31
complex	yes	1.43	0.140		0.750	20	−2.37
$E^{C}_{inter}(D_{in}) + \Delta G^{R}_{bind}(\rho,D_{in}) + \gamma\cdot\Delta SA(\rho)$							
Hs	no	1.33		0.013	0.800	20	−2.05
Hs	yes	1.39		0.014	0.750	20	−1.49
ligand/Hs	no	1.30		0.013	0.800	20	−2.16
complex	no	1.35		0.012	0.825	20	−2.33
complex	yes	1.44		0.013	0.750	20	−2.00

[a] The five rows for each binding free energy expression correspond to the five different versions of preparing the complex.

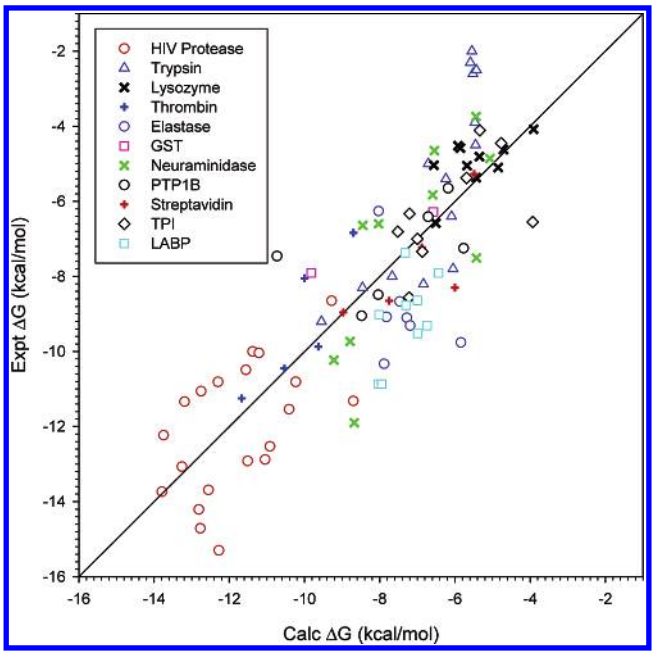

Figure 1. Scatter plot of experimental versus calculated binding affinities using eq 6.

binding affinities as the predicted value for each complex, is 2.44 kcal/mol.

Internal Dielectric Constant. Figure 2 shows a plot of the mean absolute error versus D_{in}. At each value of D_{in}, we plot the mean absolute error associated with all other parameters optimized for that value of D_{in}. We see that the errors are quite high for low values of D_{in}. The smallest errors are achieved at $D_{in} = 20$. The parameter fitting procedure drives the radii to smaller values and the solute dielectric constant to higher values. This behavior is reminiscent of the results of a recent study on pK_a calculations by Teixeira et al. in which they scanned different protein dielectric constants and four different atomic radii definitions.[27] They achieved the best agreement to experimental pK_a's using an internal dielectric of 20 and atomic radii corresponding to a

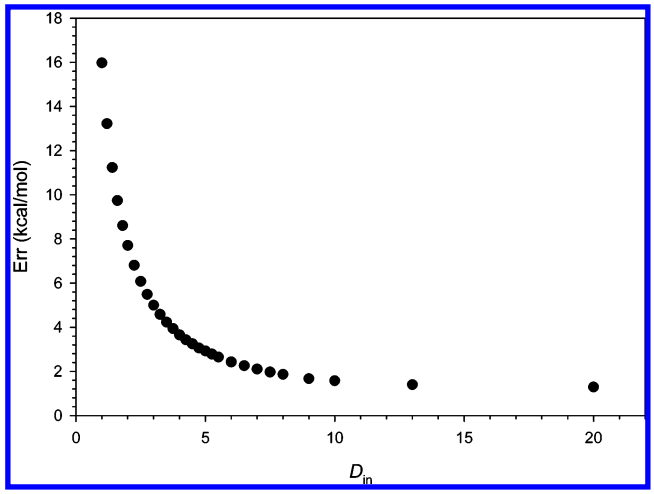

Figure 2. Mean absolute error versus D_{in}.

Lennard-Jones energy of 2RT, which are smaller than force field van der Waals radii. These two parameters, the internal dielectric constant and the atomic radii, affect the electrostatic contribution to binding. The intermolecular coulomb energy is affected by the solute dielectric constant, while the reaction field energy is affected by both parameters. The rather high value of the dielectric constant required to fit the experimental data has been observed in other studies on binding free energies.[14,28] Various explanations for the high value can be given. It has been argued that the high effective dielectric is an artifact of the rigid structures used and implicitly compensates for the lack of conformational flexibility of functional groups that can reorient their dipoles in response to the electric field.[29,30] Alternatively, the high dielectric value could also reflect the degree of water penetration in a breathing dynamic protein structure.[30−32] Another possibility is that the high D_{in}, which effectively scales the electrostatic contribution to binding, reflects part of the enthalpy−entropy compensation during binding,[33,34] as discussed further in a later section. In fact, Schapira et al.,[14] who incorporate an estimate of the change in conformational entropy in their calculations, end up with a somewhat lower value of $D_{in} = 8$ in their optimally fitted parameters. Finally, it has also been pointed out that the precise physical meaning of the dielectric constant in these continuum models is ambiguous and system-dependent.[35] Rather, the value should be left simply as a fitted parameter with at best a loose connection to a rigorous physical quantity. In any case, the optimal values for the dielectric constant found for fitting binding free energies are quite different from the range found for fitting gas-to-water hydration free energies. For the transfer free energies of neutral organic small molecules, the fitted dielectric constant falls within a broad optimum in the range of 1−4.[8] For a hydration data set of charged organic small molecules, a narrower optimum centered on $D_{in} = 1$ is obtained (see Figure S1, given as Supporting Information). In contrast, for the binding data set, the best mean absolute error obtained with dielectric constants in the range of 1−4 is 3.65 kcal/mol (Figure 2), which is more than double that of the optimum at a dielectric constant of 20. As expected, our attempts to fit the continuum electrostatic model simultaneously on both hydration and binding data have failed (not

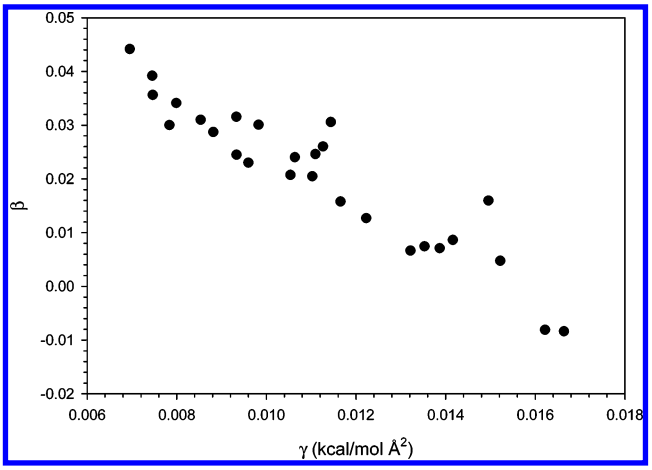

Figure 3. Scatter plot of van der Waals scaling factor versus surface area coefficient for optimized parameter combinations producing mean absolute errors less than 1.60 kcal/mol.

Table 2. Optimized Parameters with err < 1.60 kcal/mol

err	ρ	D_{in}	γ	β	C
1.29	0.8	20	0.011	0.025	−2.23
1.29	0.775	20	0.011	0.026	−2.38
1.29	0.825	20	0.011	0.024	−2.29
1.31	0.85	20	0.010	0.030	−2.15
1.32	0.75	20	0.011	0.031	−2.56
1.32	0.875	20	0.009	0.032	−2.09
1.33	0.9	20	0.010	0.023	−1.98
1.36	0.925	20	0.009	0.024	−1.88
1.38	0.95	20	0.009	0.029	−1.80
1.40	0.9	13	0.014	0.007	−1.86
1.41	0.925	13	0.013	0.007	−1.66
1.41	0.975	20	0.009	0.031	−1.73
1.41	0.875	13	0.014	0.007	−2.05
1.43	0.85	13	0.014	0.009	−2.23
1.44	1	20	0.007	0.039	−1.75
1.44	0.95	13	0.012	0.013	−1.49
1.47	1.025	20	0.008	0.034	−1.55
1.47	0.825	13	0.015	0.005	−2.31
1.48	0.975	13	0.012	0.016	−1.33
1.50	1.05	20	0.007	0.044	−1.47
1.52	1	13	0.011	0.020	−1.13
1.54	1.075	20	0.007	0.036	−1.36
1.54	0.8	13	0.015	0.016	−2.54
1.56	1.025	13	0.011	0.021	−0.96
1.56	1.1	20	0.008	0.030	−1.26
1.58	0.925	10	0.016	−0.008	−1.54
1.58	0.9	10	0.017	−0.008	−1.84

shown). This underlines the concern expressed previously about the transferability of solvation parameters obtained from transfer free energies to binding calculations.[8]

van der Waals Energy and ΔSA. The intermolecular van der Waals energy and the ΔSA are highly correlated quantities. Table 2 lists the parameter values that produce a mean absolute error of less than 1.60 kcal/mol. Figure 3 shows a scatter plot of the coefficients of the van der Waals and ΔSA terms for these low-error parameter combinations. We see a linear relationship in parameter space for these two coefficients. This arises from a correlation between the intermolecular van der Waals energy and the ΔSA. This is seen in Figure 4, which shows a scatter plot of these two quantities unscaled, with $\rho = 0.8$. It is therefore quite natural to ask if either one of these quantities by themselves would be a sufficient descriptor of the nonpolar terms. Two

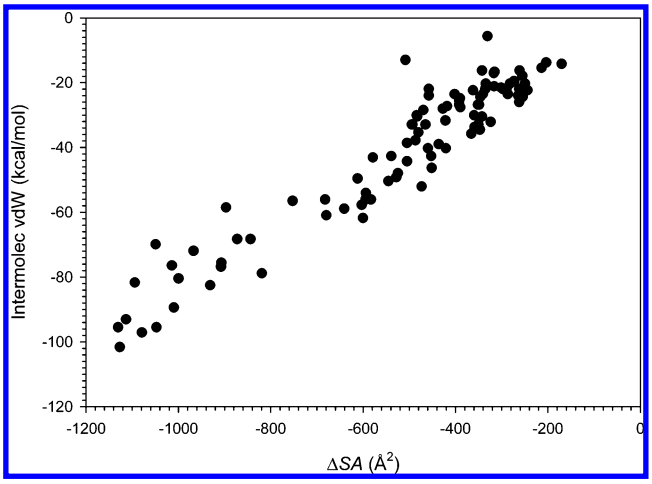

Figure 4. Scatter plot of the intermolecular van der Waals energy versus the change in surface area for the 99 protein−ligand complexes. The surface area was calculated using a radius scaling factor of 0.8, corresponding to the parameter combination yielding the lowest error.

alternative binding free energy functions were fitted to the experimental data.

$$\Delta G^{calc}_{bind}(\rho,D_{in},\beta) = E^{C}_{inter}(D_{in}) + \Delta G^{R}_{bind}(\rho,D_{in}) + \beta \cdot E^{vdw}_{inter} + C \quad (8)$$

$$\Delta G^{calc}_{bind}(\rho,D_{in},\gamma) = E^{C}_{inter}(D_{in}) + \Delta G^{R}_{bind}(\rho,D_{in}) + \gamma \cdot \Delta SA(\rho) + C \quad (9)$$

The results of the calculations are carried out on all versions of the protein−ligand complex data set and are summarized in Table 1. There is very little difference in the mean absolute error values when the nonpolar terms in the full function using eq 6 are replaced with just a surface area term in eq 9. When using just the scaled van der Waals term, there is somewhat worse error, especially for the cases where there is only limited energy minimization of the systems (versions 1 and 2 of the data set). This is understandable given the steepness of the repulsive term of the Lennard-Jones potential. The softness of the surface area term may seem to make the use of eq 9 rather than eq 6 more attractive. On the other hand, its relative insensitivity to the degree of energy refinement of the structures is both an advantage and a disadvantage. For a data set where the ligands are already properly docked with no steric clashes, we can expect the surface area term to capture the nonpolar binding contributions well. However, for poorly docked ligands with bad steric clashes, such a binding free energy function would not penalize misdocked configurations sufficiently.

The binding affinity model in eq 6 can be expanded by replacing the uniform surface area term with atom-type-dependent surface area coefficients to account for differences in solute−solvent van der Waals interactions as well as for other contributions to solvation and binding that are not captured by molecular mechanics force fields and continuum electrostatic models. Our initial results indicate that the incorporation of such surface-based atomic potentials can lead to substantial improvements to the overall fit of our binding affinity scoring function (see Figure S2, given as Supporting Information).

Molecular Size. It has been observed in other studies that for some targets molecular size alone as a descriptor can

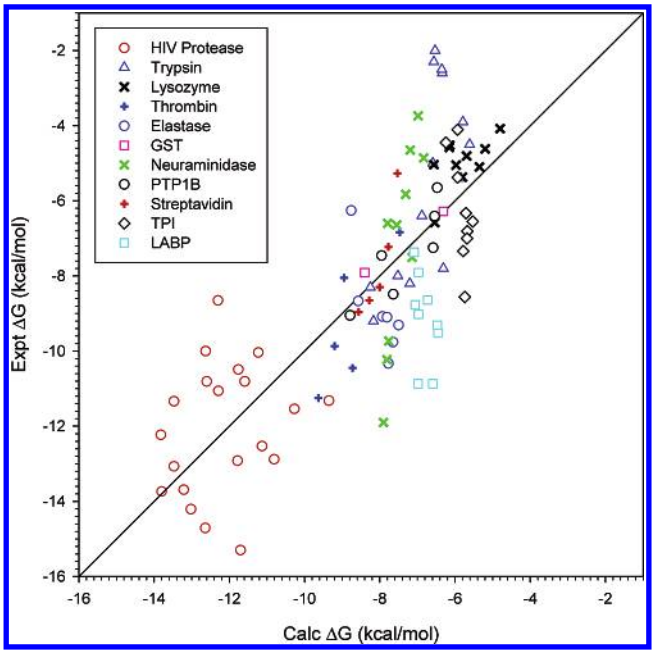

Figure 5. Scatter plot of experimental versus calculated binding affinities using eq 10.

capture much of the trend in binding affinity data.[36] Since ligand size is correlated with ΔSA, we explored the use of just ΔSA as a predictor of binding affinity.

$$\Delta G_{\text{bind}}^{\text{calc}}(\gamma) = \gamma \cdot \Delta\text{SA} + C \qquad (10)$$

The optimal fitted parameters obtained were $\rho = 0.775$, $\gamma = 0.00939$ kcal/mol·Å^2, and $C = -3.25$ kcal/mol with a mean absolute error of 1.48 kcal/mol. Figure 5 shows a scatter plot of the experimental versus calculated binding free energies using eq 10. Indeed, the overall fit does not seem much worse than the more sophisticated model using eq 6. However, there are deficiencies in this model that are not captured by the overall mean absolute error. Although the overall fit for the whole set is good, for a number of targets such as neuraminidase, LABP, and TPI, there is virtually no predictive value in the model. The calculated binding free energies do not change much despite the several kilocalories per mole range in experimental values. For each of these targets, the ligands are approximately the same size and hence lead to little variation in ΔSA. The Spearman $R = 0.782$, which is somewhat worse than the 0.854 observed when using eq 6. However, the difference in overall Spearman R value does not capture the much worse intra-target correlations observed in Figure 5 as compared to that in Figure 1.

Because of the large influence of molecular size on the absolute binding free energies, we clustered the ligands into three molecular weight ranges (<200, 200−450, >450) and calculated the Spearman R correlation for experimental versus calculated binding free energies within each range. The three ranges had 33, 31, and 35 ligands, respectively. Figure 6a and b are replots of the data in Figures 1 and 5 with the symbols assigned according to the molecular weights of the ligands. We see more clearly the much poorer predictive value of the ΔSA-only scoring function. The effect is most visible for the lower-molecular-weight ligands where the variation in molecular weights is less. We see much greater clustering of calculated binding affinity according to molecular size in Figure 6b versus that in Figure 6a. Table 3 summarizes the resulting Spearman R values for the scatter plots in Figures 1 and 5. We note that the Spearman R value now better reflects the deterioration in rank correlation, particularly for the low-molecular-weight ligands. The deterioration of predictive value in Figure 6b is due to the loss of electrostatic information. This is seen clearly in Figure 6c in which the ΔSA term is supplemented by the electrostatic term using eq 9.

Scaling of the Intermolecular van der Waals Energy. The intermolecular energy has to be scaled down significantly in order to obtain a good fit to experimental binding affinity data. If we use unscaled van der Waals energies and adjust the other parameters to best fit the experimental data, we obtain a mean unsigned error of 5.1 kcal/mol. This is about 3 times larger than the error when the van der Waals energies are scaled and worse than the null hypothesis error of 2.44 kcal/mol. The significant scaling of gas-phase molecular mechanics (MM) force-field-based energies required in order to reproduce binding affinities in solution has been observed previously. The most notorious and best investigated is the case of the linear interaction energy (LIE) method using molecular dynamics simulations with an explicit solvent.[5] Recently, it has been shown that an efficient LIE-like approach using MM-energy-minimized single structures and continuum solvation also requires heavy scaling of intermolecular van der Waals energies.[37] Scaling-down relative to the gas-phase force-field-based van der Waals potentials was also observed in order to reproduce experimental data on protein stability in solution.[38] Several hypotheses have been raised to explain possible causes for this behavior.[38−40]

Our initial thought was that the scaling was merely reflecting the loss of ligand−water van der Waals interactions upon binding to the protein. However, this loss of ligand−water nonelectrostatic interaction energy should already be largely captured by the surface area coefficient. To demonstrate this, we examined the experimental gas-to-water transfer free energies of hydrocarbons in which the free energies arise predominantly from the balance of the cost of cavity formation and the gain of solute−water van der Waals interactions, that is, minimal solute−solvent electrostatic contribution. Linear regression of the experimental hydration free energies versus molecular surface area for a series of acyclic alkanes yields a surface area coefficient of 0.010 kcal/mol·Å^2 (data not shown). This is close to the optimized value of $\gamma = 0.011$ kcal/mol·Å^2 in our binding models. Hence, the scaling of the intermolecular van der Waals interaction must be compensating for some other component of the total free energy that is missing in our free energy expression, eq 6. A possible candidate for the missing term is the change in configurational entropy of the ligand and protein upon complex formation.

Scaling Coefficients and Enthalpy−Entropy Compensation. In binding simulations involving small model systems, Gilson and co-workers[33,34] find a marked anticorrelation between the change in average potential energy plus solvation, $\Delta\langle U+W\rangle$, and the change in configurational entropy, ΔS, upon binding. They observe that the (configurational) entropic cost of binding arises from a narrowing of the energy wells available to the complex as compared to the free states.

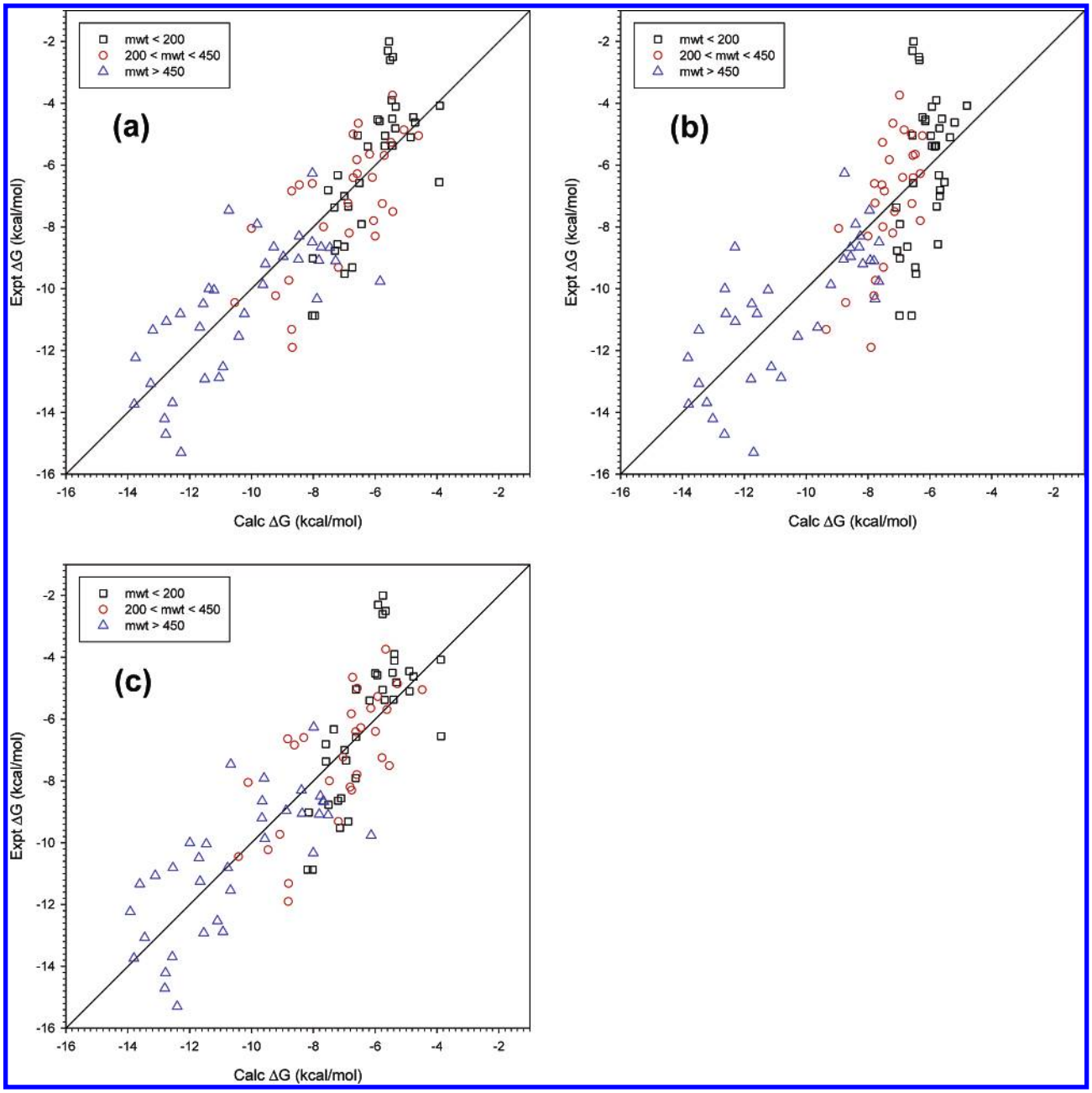

Figure 6. Scatter plots with symbols assigned according to the molecular weights of the ligands: (a) same data as Figure 1, (b) same data as Figure 5, (c) based on eq 9.

Table 3. Spearman *R* Coefficients for Various Ligand Molecular Weight Ranges

scoring function	MW < 250	250 < MW < 450	450 < MW < 800
eq 6	0.764	0.666	0.767
eq 10	0.347	0.651	0.713

In Figure 11 of Gilson et al.,[34] we see that approximately 90% of $\Delta\langle U+W\rangle$ is canceled out by the unfavorable change in entropy. This high degree of compensation suggests that the strong scaling of the van der Waals and electrostatic terms (through small β and high D_{in}, respectively) in the present work has its origins in entropic terms that are missing in our binding free energy function. As noted by Gilson et al., simply scaling down the computed change in energy could crudely account for the proportional loss in entropy.[34] This essentially substitutes a scaled $-\Delta\langle U+W\rangle$ for the configurational entropy term. Of course, the enthalpy−entropy anticorrelation is not perfect, and the resulting scatter in ΔG_{bind} versus the solvated potential energy is magnified as seen in Figure 9 of Gilson et al.[34] Nevertheless, in the absence of an explicit configurational entropy calculation, it is a useful approximation to the absolute binding free energy.

We therefore explored the following functional form for the binding free energy

$$\Delta G^{calc}_{bind}(\rho,D_{in},\alpha,\gamma,C) = \alpha[E^{C}_{inter}(D_{in}) + \Delta G^{R}_{bind}(\rho,D_{in}) + E^{vdw}_{inter} + \gamma\cdot\Delta SA(\rho)] + C \quad (11)$$

where the entire potential energy plus solvation is scaled by a fitting coefficient, α. Furthermore, we used a fixed $\gamma = 0.010$ kcal/mol·Å^2, by fitting to hydration free energies of a series of acyclic alkanes. Optimization of the parameters against our data set of 99 protein complexes yields $\alpha = 0.104$, $D_{in} = 3.25$, $\rho = 1.1$, and $C = -2.76$ kcal/mol. The

mean absolute error is 1.38 kcal/mol, and the Spearman $R = 0.79$. The overall scaling factor of 0.104 for the energy is similar to the 90% enthalpy−entropy compensation observed by Gilson and co-workers in their studies using extensive conformational sampling.[34] This supports the interpretation of the entropic origin of the scaling coefficients. In the framework of eq 6, we note that the coefficients obtained for eq 11 yield an effective D_{in}, $D_{in}^{eff} \approx D_{in}/\alpha = 32.5$. (This is not exact because the dependence of the reaction field energy on D_{in} is more complicated than a linear scaling; see the next section.) These results suggest that electrostatic interactions in protein−ligand binding can in fact be described by a low $D_{in} = 3.25$ but that the high effective D_{in} values obtained by fitting computed single-point energies to experimental free energies are largely an artifact of the missing enthalpy−entropy compensation in single-point calculations. From an aesthetic perspective, eq 11 is more satisfying than eq 6 because it remains closer to being an interpretable physics-based binding free energy function while eq 6 drifts more toward being a regression against a set of physical descriptors. It is worth reiterating, though, that the α-scaling factor can only crudely capture the average trend of the entropy component. Its sole purpose is to rescale the calculated sum of energy terms into the range of experimentally observed binding free energies. The lack of an explicit entropy term likely contributes to the scatter in the predicted versus experimental binding free energies.

Direct experimental verification of the $\Delta\langle U+W\rangle - \Delta S_{config}$ compensation against experimental binding data is not straightforward because it is not possible to decouple the solvation entropy contributions from the total measured entropy changes in order to obtain just the configurational entropy. Perhaps the closest relevant system comes from the work of Searle and Williams who plotted literature data for ΔH against the $T\Delta S$ of fusion at 300 K for 21 organic compounds.[41] We can take fusion to be the analog of the binding step. This system does not have the solvation entropy associated with aqueous binding experiments and allows us to focus on the enthalpy−entropy compensation related to the reduction of conformational flexibility upon fusion. They found enthalpy−entropy compensation that could be fitted by the equation $y = -2.2 + 1.3x$ for ΔH versus $T\Delta S$ with a Pearson correlation coefficient $R = 0.89$. This means that approximately 77% of the enthalpic contribution is canceled out by the loss in configurational entropy. The degree of compensation is similar to, albeit somewhat smaller than, the 90% observed in the theoretical binding free energy studies of Gilson et al.[34]

Conductor-Limit Approximation. The most expensive computational step in the parametrization is the calculation of the reaction field energies at various combinations of D_{in} and ρ. In this work, we scanned 29 different D_{in} values for each of the 15 values of ρ. One way to speed up this step of the calculation is to use the conductor-limit approximation for the solvent dielectric, that is, $D_{out} = \infty$.[42] The conductor limit is a good approximation of water as a solvent and is used in quantum mechanics calculations with continuum solvation.[42−45] In the boundary element method, the reaction field energy is proportional to the surface charge density, σ, which is computed from a large linear system of equations[10,11,46,47]

$$(\mathbf{I} - f\mathbf{K})\boldsymbol{\sigma} = f\mathbf{E} \tag{12}$$

where $f = (D_{in} - D_{out})/(D_{in} + D_{out})$. **I** is the identity matrix, and **K** depends solely on molecular geometry. **E** is the normal component of the electric field at the molecular surface and scales like $1/D_{in}$. When $D_{out} = \infty$, the reaction field energy depends on D_{in} alone. Hence, by calculating the reaction field energy at $D_{in} = 1$, we can obtain the energy at another value of D_{in} simply by scaling by $1/D_{in}$ rather than re-solving the system of equations. The results of the parametrization are largely unaltered by this approximation. Using the same parameter scanning protocol described above, we obtain similar optimized parameters ($D_{in} = 20$, $\beta = 0.036$, $\gamma = 0.0077$, $C = -2.51$, and $\rho = 1.1$) with a mean absolute error of 1.38 kcal/mol, slightly worse than that with $D_{out} = 78.5$. Our optimal D_{in} values always seem to be at the edge of our scanned range of values for D_{in}. One may ask if the error keeps decreasing as we increase D_{in}. One advantage of using $D_{out} = \infty$ is that D_{in} can now be treated as a continuous variable to be optimized rather than a discrete parameter to be scanned. Optimal parameters using a continuous D_{in} yield the combination ($D_{in} = 29.7$, $\beta = 0.034$, $\gamma = 0.0072$, $C = -2.88$, and $\rho = 1.1$) with a mean absolute error of 1.35 kcal/mol. We see the presence of a minimum-error value rather than a monotonic decrease in error with an increasing D_{in}. This is reminiscent of the work of Teixeira et al. in which they observe optimum D_{in} values in the range of 20−30 when fitting pK_a values using various definitions of atomic radii.[27]

The data set of 99 protein−ligand complexes used above consists entirely of protein−ligand pairs with net charges of the same sign or with at least one of the pair having zero net charge. With a D_{out} of 78.5, we were unable to find a set of parameters that would adequately fit the experimental data if we also included complexes in which the protein and ligand had opposite net charges (Figure S3a, Supporting Information). One fortunate side effect of the conductor-limit approximation is that we are now able to obtain parameters that simultaneously provide good fits for protein−ligand pairs of opposite or like net charges (Figure S3b, Supporting Information). The reason for this has to do with the relative signs of the coulomb and reaction field contributions and their functional dependence on the value of D_{in}.[14] The problem appears to be mitigated by having the coulomb and reaction field energies scaled in the same way by D_{in}.

Applicability to Virtual Screening. One of the main goals of this work is to develop a scoring function for use in a virtual screening pipeline. As an illustration of the usefulness of the SIE function, we carried out enrichment studies, that is, finding true hits embedded in a collection of decoys, of two targets not included in our training set. We used the ER and TK decoy sets of Bissantz et al.[48] These decoy sets consist of 990 random molecules and 10 known binders for each of the targets. The test is to see whether the known binders are ranked highly by the scoring function relative to the decoys in a virtual screening calculation. The process requires the generation of poses for each ligand that will be scored using the SIE function. The details of the docking procedure and virtual screening pipeline will be described in detail in a future paper. Briefly, energy-refined structures

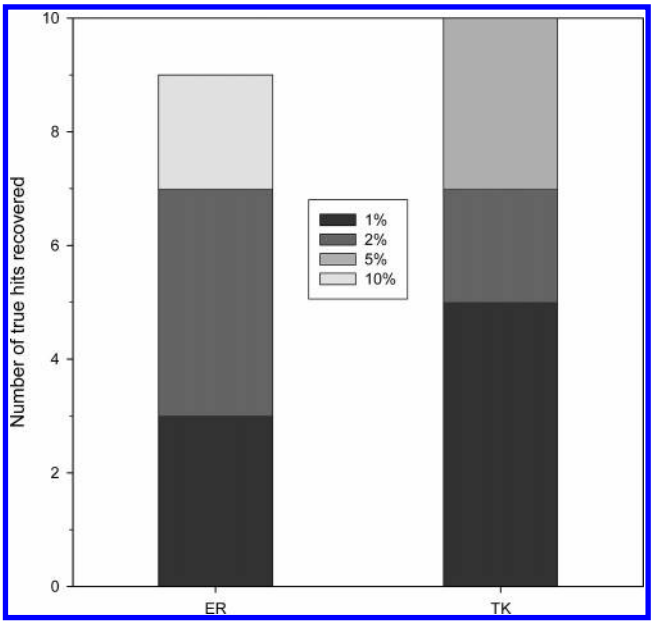

Figure 7. Enrichment results for ER and TK. Each target has 10 true hits and 990 decoys. Four shades of gray in decreasing darkness in the chart represent the number of hits within the top 1, 2, 5, and 10%, respectively. Parameters are taken from Figure S3b in the Supporting Information.

for ER and TK were prepared from their respective crystal structures. We then used FRED and OMEGA (OpenEye Scientific Software, Inc., Santa Fe, NM) to generate poses for each ligand. The protein structures were kept rigid during the docking step. The poses were filtered using a simplified scoring function incorporating shape and hydrogen-bonding terms and the ligands subsequently energy-refined in the rigid protein binding site. The top 10 poses were then scored using the SIE function, and the lowest-energy pose was retained.

The results of the enrichment study are summarized in Figure 7. Shown are the number of true hits recovered in the top 1, 2, 5, and 10% of the top-scoring ligands. For ER, seven of the true hits are recovered in the top 2% and nine are recovered in the top 10%. For TK, five of the true hits are recovered in the top 1% and all 10 in the top 10%. ER is considered to be an easy case because the true hits in the set are nanomolar inhibitors. In TK, only two true hits are submicromolar, while the rest range from 2 to 200 micromolar. Table 4 summarizes the predicted binding free energies and ranks of the true hits. It is a measure of success to find that the range of predicted absolute binding free energies for the true hits is consistent with the range of known activities of these compounds. Also shown in Table 4 are the predicted energies and ranks of the true hits if a surface-area-based function alone is used. For ER, in which the interactions are mainly hydrophobic, we still recover nine true hits in the top 10%. But for TK, which involves polar interactions, the true hits are ranked near the bottom of the list.

The SIE function is too expensive computationally to be used directly in the docking and early filtering of ligand poses. However, in the later stages of scoring prefiltered poses, it is quite feasible to use it even for large data sets (>100 000 compounds). The most expensive part of the SIE function is the calculation of the change in reaction field energy. When the program BRI BEM is used,[10,11] it takes on average under 25 s to calculate the reaction field energy

Table 4. Predicted Absolute Binding Free Energies and Relative Ranks of True Binders of ER and TK[a]

full SIE function (eq 6)				surface area term only (eq 10)			
ER		TK		ER		TK	
ΔG	rank	ΔG	rank	ΔG	rank	ΔG	rank
−10.73	1	−7.45	1	−11.73	1	−7.12	967
−10.33	3	−7.33	2	−11.39	2	−7.12	968
−10.18	6	−7.28	3	−10.34	27	−7.12	969
−9.93	12	−7.03	5	−10.14	42	−7.01	980
−9.90	13	−6.90	8	−9.96	59	−6.97	986
−9.77	14	−6.86	11	−9.90	67	−6.91	990
−9.64	17	−6.81	13	−9.89	68	−6.90	992
−9.13	52	−6.61	23	−9.76	99	−6.77	995
−8.99	69	−6.50	33	−9.37	215	−6.70	996
−8.39	212	−6.46	34	−9.19	287	−6.61	997

[a] All energies are in kcal/mol. For each of the targets, there are 10 true binders and 990 decoys taken from Bissantz et al.[48] Parameters for the full SIE function are the same as those in Figure 7.

of a typical 200-residue protein−ligand complex on a single 2.8 GHz Xeon processor. In a virtual screening pipeline, this time is reduced further when the same target is used repeatedly on a library of ligands.

Degeneracy of Parameters. Although we report a particular combination of parameters that best reproduces experimental binding affinities, there is a range of parameter combinations that gives essentially equally good fits. We have already seen, above, the linear correlation between the van der Waals scaling factor, β, and the surface area coefficient, γ. Similarly, as seen in Table 2, practically the full range of scanned radius-scaling factors is acceptable in combination with a corresponding value of D_{in}. The mathematically optimal parameters reported in Table 1 pertain specifically to the data set used in calibration. The optimal parameters will undoubtedly change for an altered or expanded data set. However, the existence of a relatively flat valley in parameter space in the vicinity of the optimum suggests that there is a fair amount of leeway in adjusting the parameters to fit an extended set while maintaining a good fit to the existing data set. The existence of multiple sets of parameters with a similar quality of fit has been observed by other workers as well.[9,14] In a future paper on virtual screening applications, we will explore fine-tuning of the parameters to obtain optimal performance in enrichment tests.

CONCLUSION

In this work, we presented a binding free energy function that consists of force field terms supplemented by solvation terms. We used this function to calibrate the solvation model along with the binding interaction terms in a self-consistent manner. The motivation for this approach was that the solute dielectric constant-dependence of calculated hydration gas-to-water transfer free energies is markedly different from that of binding free energies. Hence, we sought to calibrate directly the solvation terms in the context of a binding calculation. The parameters of the model were optimized to best reproduce the absolute binding free energies for a set of 99 protein−ligand complexes. The fitting results in a mean unsigned error of 1.29 kcal/mol in the predicted binding affinity. We find that the fitting drives the effective solute dielectric constant to high values. We also find that the

intermolecular van der Waals energy has to be scaled strongly. The origin of both the high effective solute dielectric constant and the strong van der Waals scaling appears to be entropy−enthalpy compensation in binding. The introduction of a conductor model ($D_{out} = \infty$) for the solvent speeds up the calculation of the reaction field energy at various values of D_{in} and resolves the difficulty to simultaneously fit experimental data for protein−ligand complexes of like and opposite charges within the same parameter set at least for the two examples tested here. The relative flatness of the parameter space around the minimum suggests the capability to fine-tune the free energy function for other data sets and/or constraints while retaining the good fit with the current data set.

The test data set used consisted of five different ways of preparing the protein−ligand complexes, representing various levels of energy refinement and the presence or absence of explicit water molecules. This database of diverse protein−ligand complexes will be useful for benchmarking and scoring function development studies in other laboratories (see the Supporting Information for availability). A notable finding in our own work is that the presence of explicit bound water in the final protein structure used for calculating binding affinities is not required to obtain good agreement with experimental results. It is possible, as pointed out by a reviewer, that explicit bound water molecules may still be necessary for docking calculations. However, our limited docking studies (Supporting Information, Figure S4) suggest that a continuum solvent model may be sufficient for docking as well.

ACKNOWLEDGMENT

S.B. was partly supported by a grant from the Protein Engineering Network of Centres of Excellence (PENCE). We thank E. Smiley for assistance in gathering literature references for binding constants. We are grateful to OpenEye Scientific Software, Inc., for providing a copy of FRED and OMEGA. This is NRCC publication number 47544.

Supporting Information Available: Additional figures comprised of (1) comparison of the (ρ, D_{in}) dependence of hydration transfer free energies of small molecules versus binding free energies, (2) preliminary data on the inclusion of atom-type-dependent surface area terms in the binding free energy function, (3) effect of $D_{out} = \infty$ on parameter fitting, and (4) two test cases illustrating the ability to discriminate docked and misdocked poses. This information is available free of charge via the Internet at http://pubs.acs.org. The mol2 files of all the complexes (five versions) listed in Table S1 of the Supporting Information and the corresponding experimental binding affinity data with the literature references are available for download at http://www2.bri.nrc.ca/ccb/supp/jcim2006.html.

REFERENCES AND NOTES

(1) Tokarski, J. S.; Hopfinger, A. J. Prediction of Ligand-Receptor Binding Thermodynamics by Free Energy Force Field (FEFF) 3D-QSAR Analysis: Application to a Set of Peptidometic Renin Inhibitors. *J. Chem. Inf. Comput. Sci.* **1997**, *37*, 792−811.

(2) Kollman, P. A.; Massova, I.; Reyes, C.; Kuhn, B.; Huo, S.; Chong, L.; Lee, M.; Lee, T.; Duan, Y.; Wang, W.; Donini, O.; Cieplak, P.; Srinivasan, J.; Case, D. A.; Cheatham, T. E. Calculating Structures and Free Energies of Complex Molecules: Combining Molecular Mechanics and Continuum Models. *Acc. Chem. Res.* **2000**, *33*, 889−897.

(3) Gohlke, H.; Klebe, G. Approaches to the Description and Prediction of the Binding Affinity of Small-Molecule Ligands to Macromolecular Receptors. *Angew. Chem., Int. Ed.* **2002**, *41*, 2644−2676.

(4) Gohlke, H.; Klebe, G. Statistical Potentials and Scoring Functions Applied to Protein−Ligand Binding. *Curr. Opin. Struct. Biol.* **2001**, *11*, 231−235.

(5) Åqvist, J.; Luzhkov, V. B.; Brandsdal, B. O. Ligand Binding Affinities from MD Simulations. *Acc. Chem. Res.* **2002**, *35*, 358−365.

(6) Simonson, T.; Archontis, G.; Karplus, M. Free Energy Simulations Come of Age: Protein−Ligand Recognition. *Acc. Chem. Res.* **2002**, *35*, 430−437.

(7) Kitchen, D. B.; Decornez, H.; Furr, J. R.; Bajorath, J. Docking and Scoring in Virtual Screening for Drug Discovery: Methods and Applications. *Nat. Rev. Drug Discovery* **2004**, *3*, 935−949.

(8) Rankin, K. N.; Sulea, T.; Purisima, E. O. On the Transferability of Hydration-Parametrized Continuum Electrostatics Models to Solvated Binding Calculations. *J. Comput. Chem.* **2003**, *24*, 954−962.

(9) Zou, X.; Sun, Y.; Kuntz, I. D. Inclusion of Solvation in Ligand Binding Free Energy Calculations Using the Generalized-Born Model. *J. Am. Chem. Soc.* **1999**, *121*, 8033−8043.

(10) Purisima, E. O. Fast Summation Boundary Element Method for Calculating Solvation Free Energies of Macromolecules. *J. Comput. Chem.* **1998**, *19*, 1494−1504.

(11) Purisima, E. O.; Nilar, S. H. A Simple yet Accurate Boundary Element Method for Continuum Dielectric Calculations. *J. Comput. Chem.* **1995**, *16*, 681−689.

(12) Cornell, W. D.; Cieplak, P.; Bayly, C. I.; Gould, I. R.; Merz, K. M., Jr.; Ferguson, D. M.; Spellmeyer, D. C.; Fox, T.; Caldwell, J. W.; Kollman, P. A. A Second Generation Force Field for the Simulation of Proteins, Nucleic Acids, and Organic Molecules. *J. Am. Chem. Soc.* **1995**, *117*, 5179−5197.

(13) Roche, O.; Kiyama, R.; Brooks, C. L., III. Ligand-Protein DataBase: Linking Protein−Ligand Complex Structures to Binding Data. *J. Med. Chem.* **2001**, *44*, 3592−3598.

(14) Schapira, M.; Totrov, M.; Abagyan, R. Prediction of the Binding Energy for Small Molecules, Peptides and Proteins. *J. Mol. Recognit.* **1999**, *12*, 177−190.

(15) Word, J. M.; Lovell, S. C.; Richardson, J. S.; Richardson, D. C. Asparagine and Glutamine: Using Hydrogen Atom Contacts in the Choice of Side-Chain Amide Orientation. *J. Mol. Biol.* **1999**, *285*, 1735−1747.

(16) Wang, J.; Wolf, R. M.; Caldwell, J. W.; Kollman, P. A.; Case, D. A. Development and Testing of a General Amber Force Field. *J. Comput. Chem.* **2004**, *25*, 1157−1174.

(17) Bayly, C. I.; Cieplak, P.; Cornell, W. D.; Kollman, P. A. A Well-Behaved Electrostatic Potential Based Method Using Charge Restraints for Deriving Atomic Charges: The RESP Model. *J. Phys. Chem.* **1993**, *97*, 10269−10280.

(18) Schmidt, M. W.; Baldridge, K. K.; Boatz, J. A.; Elbert, S. T.; Gordon, M. S.; Jensen, J. H.; Koseki, S.; Matsunaga, N.; Nguyen, K. A.; Su, S.; Windus, T. L.; Dupuis, M.; Montgomery, J. A., Jr. General Atomic and Molecular Electronic Structure System. *J. Comput. Chem.* **1993**, *14*, 1347−1353.

(19) Jakalian, A.; Bush, B. L.; Jack, D. B.; Bayly, C. I. Fast, Efficient Generation of High-Quality Atomic Charges. AM1-BCC Model: I. Method. *J. Comput. Chem.* **2000**, *21*, 132−146.

(20) Åqvist, J. Ion-Water Interaction Potentials Derived from Free Energy Perturbation Simulations. *J. Phys. Chem.* **1990**, *94*, 8021−8024.

(21) Chan, S. L.; Purisima, E. O. Molecular Surface Generation Using Marching Tetrahedra. *J. Comput. Chem.* **1998**, *19*, 1268−1277.

(22) Bhat, S.; Purisima, E. O. Molecular Surface Generation Using a Variable-Radius Solvent Probe. *Proteins: Struct., Funct., Bioinf.* **2006**, *62*, 244−261.

(23) Pitarch, J.; Moliner, V.; Pascual-Ahuir, J. L.; Silla, E.; Tuñón, I. Can Hydrophobic Interactions Be Correctly Reproduced by the Continuum Models? *J. Phys. Chem.* **1996**, *100*, 9955−9959.

(24) Dowdy, S.; Weardon, S.; Chilko, D. *Statistics for Research*; John Wiley & Sons, Inc.: Hoboken, NJ, 2004; pp 250−252.

(25) R Development Core Team. *R: A Language and Environment for Statistical Computing*; R Foundation for Statistical Computing: Vienna, Austria, 2005. http://www.R-project.org (accessed Nov 20, 2006).

(26) Wang, R.; Lu, Y.; Fang, X.; Wang, S. An Extensive Test of 14 Scoring Functions Using the PDBbind Refined Set of 800 Protein−Ligand Complexes. *J. Chem. Inf. Comput. Sci.* **2004**, *44*, 2114−2125.

(27) Teixeira, V. H.; Cunha, C. A.; Machuqueiro, M.; Oliveira, A. S. F.; Victor, B. L.; Soares, C. M.; Baptista, A. M. On the Use of Different Dielectric Constants for Computing Individual and Pairwise Terms in Poisson-Boltzmann Studies of Protein Ionization Equilibrium. *J. Phys. Chem. B* **2005**, *109*, 14691−14706.

(28) Zhou, Y.; Abagyan, R. How and Why Phosphotyrosine-Containing Peptides Bind to the SH2 and PTB Domains. *Folding Des.* **1998**, *3*, 513−522.

(29) Simonson, T.; Brooks, C. L., III. Charge Screening and the Dielectric Constant of Proteins: Insights from Molecular Dynamics. *J. Am. Chem. Soc.* **1996**, *118*, 8452−8458.
(30) Garcia-Moreno, B. E.; Dwyer, J. J.; Gittis, A. G.; Lattman, E. E.; Spencer, D. S.; Stites, W. E. Experimental Measurement of the Effective Dielectric in the Hydrophobic Core of a Protein. *Biophys. Chem.* **1997**, *64*, 211−224.
(31) Woodward, C. Is the Slow-Exchange Core the Protein Folding Core? *Trends Biochem. Sci.* **1993**, *18*, 359−360.
(32) Dong, F.; Vijayakumar, M.; Zhou, H. X. Comparison of Calculation and Experiment Implicates Significant Electrostatic Contributions to the Binding Stability of Barnase and Barstar. *Biophys. J.* **2003**, *85*, 49.
(33) Chang, C. E.; Gilson, M. K. Free Energy, Entropy, and Induced Fit in Host-Guest Recognition: Calculations with the Second-Generation Mining Minima Algorithm. *J. Am. Chem. Soc.* **2004**, *126*, 13156−13164.
(34) Chen, W.; Chang, C. E.; Gilson, M. K. Calculation of Cyclodextrin Binding Affinities: Energy, Entropy, and Implications for Drug Design. *Biophys. J.* **2004**, *87*, 3035−3049.
(35) Schutz, C. N.; Warshel, A. What Are the Dielectric "Constants" of Proteins and How To Validate Electrostatic Models? *Proteins* **2001**, *44*, 400−417.
(36) Ferrara, P.; Gohlke, H.; Price, D. J.; Klebe, G.; Brooks, C. L., III. Assessing Scoring Functions for Protein−Ligand Interactions. *J. Med. Chem.* **2004**, *47*, 3032−3047.
(37) Huang, D.; Caflisch, A. Efficient Evaluation of Binding Free Energy Using Continuum Electrostatics Solvation. *J. Med. Chem.* **2004**, *47*, 5791−5797.
(38) Lomize, A. L.; Reibarkh, M. Y.; Pogozheva, I. D. Interatomic Potentials and Solvation Parameters from Protein Engineering Data for Buried Residues. *Protein Sci.* **2002**, *11*, 1984−2000.
(39) Wang, W.; Wang, J.; Kollman, P. A. What Determines the van der Waals Coefficient β in the LIE (Linear Interaction Energy) Method to Estimate Binding Free Energies Using Molecular Dynamics Simulations? *Proteins* **1999**, *34*, 395−402.
(40) Sham, Y. Y.; Chu, Z. T.; Tao, H.; Warshel, A. Examining Methods for Calculations of Binding Free Energies: LRA, LIE, PDLD-LRA, and PDLD/S-LRA Calculations of Ligands Binding to an HIV Protease. *Proteins* **2000**, *39*, 393−407.
(41) Searle, M. S.; Williams, D. H. The Cost of Conformational Order: Entropy Changes in Molecular Associations. *J. Am. Chem. Soc.* **1992**, *114*, 10690−10697.
(42) Klamt, A. Conductor-Like Screening Model for Real Solvents: A New Approach to the Quantitative Calculation of Solvation Phenonmena. *J. Phys. Chem.* **1995**, *99*, 2224−2235.
(43) Klamt, A.; Schüürmann, G. COSMO: A New Approach to Dielectric Screening in Solvents with Explicit Expressions for the Screening Energy and Its Gradient. *J. Chem. Soc., Perkin Trans. 2* **1993**, 799−805.
(44) Cossi, M.; Rega, N.; Scalmani, G.; Barone, V. Energies, Structures, and Electronic Properties of Molecules in Solution with the C-PCM Solvation Model. *J. Comput. Chem.* **2003**, *24*, 669−681.
(45) Takano, Y.; Houk, K. N. Benchmarking the Conductor-Like Polarizable Continuum Model (CPCM) for Aqueous Solvation Free Energies of Neutral and Ionic Organic Molecules. *J. Chem. Theory Comput.* **2005**, *1*, 70−77.
(46) Zauhar, R. J.; Morgan, R. S. The Rigorous Computation of the Molecular Electric Potential. *J. Comput. Chem.* **1988**, *9*, 171−187.
(47) Zauhar, R. J.; Morgan, R. S. A New Method for Computing the Macromolecular Electric Potential. *J. Mol. Biol.* **1985**, *186*, 815−820.
(48) Bissantz, C.; Folkers, G.; Rognan, D. Protein-Based Virtual Screening of Chemical Databases. 1. Evaluation of Different Docking/Scoring Combinations. *J. Med. Chem.* **2000**, *43*, 4759−4767.

CI600406V